The effect of thermal fluctuations on elastic instabilities of biopolymers

Emanuel, M.D.

Chapter 7

Thermal Fluctuations and the Multi-Plectoneme Phase

To account for thermal fluctuations two strategies seem to dominate the theoretical considerations in the literature. They both do not consider the fluctuations per se in the plectoneme, but either conclude that plectoneme formation hardly affects the thermal fluctuations [150] or boldly consider the shortening only happening in the tails [176, 177]. Both approaches have their shortcomings.

In the first case, it not clear why the size of the thermal fluctuations inside the plectoneme should be the same as in the tails. The confinement of the chain in the plectoneme is the result of a subtle equilibrium between the applied tension, the electrostatic repulsion and the need to reduce the twist through writhe. Furthermore this procedure needs an extra surface charge reduction of the chain to reproduce experimental slopes [150].

The second approach, when properly applied, does not need this ad hoc charge reduction to get a reasonable agreement with some of the experiments but has the conceptual problem that there is no a priori reason why the plectoneme would be totally immune to fluctuations. The reasoning that thermal fluctuations are small within the plectoneme and thus can be ignored is erroneous since the plectoneme free energy has to be compared with the plectonemeless configuration where the finite fluctuations have a known dependence on tension and applied torque. The only conclusion one can draw, following this line of thought, is that the extreme reduction in the number of configurations prohibits plectoneme formation.

The influence of thermal fluctuations on free energy, extension and twist for linking numbers below the plectoneme transition are pretty well understood [172, 173]. This result can not be used within a plectoneme. That is why the free energy of the tails is often taken as the free energy of a worm-like chain under tension, not taking the effect of a constraint nonzero linking number into account, or alternatively putting all linking number dependence in an effective torsional stiffness [151] after a low torque expansion. The problem remains in that

there is no reason to assume that this effective torsional stiffness can be used within the plectoneme to account for the torsional part of the free energy.

We are using a detailed calculation of a confined worm-like chain under torsion. Our strategy is to integrate out short wavelength degrees of freedom, restricted to fluctuations around the straight chain and plectoneme solutions, treating the tails and the plectoneme separately. We will then calculate the free energy of the resulting effective Hamiltonian as a sum over the local minima.

7.1 Short wave length fluctuations

Below the transition we use the results from Moroz and Nelson [172] extended with with a finite stretch modulus and twist stretch coupling as performed in Section 6.1. Comparing the expression for the free energy (6.13) with the calculations from [172], we see that (the inverse of) their expansion parameter K is replaced by:

$$\mathrm{K} = \sqrt{\mathrm{f}\,\mathrm{P_b} - (\pi\,\mathrm{P_c}'\,\mathrm{lk} + \frac{\mathrm{B\,f}}{2\,\mathrm{S}})^2} \tag{7.1}$$

The free energy density of the chain expressed in this factor can now be written as (6.13):

$$\begin{aligned} \mathfrak{f}_{\mathrm{tail}} &= 2\pi^2\,\mathrm{P_c}\,\mathrm{lk}^2 - \frac{(\mathrm{f} - 2\pi\,\mathrm{B}\,\mathrm{lk})^2}{2\,\mathrm{S}} - \mathrm{f} + \frac{\mathrm{K}}{\mathrm{P_b}}\left(1 - \frac{1}{4\,\mathrm{K}} - \frac{1}{64\,\mathrm{K}^2}\right) \\ &\simeq \mathfrak{f}^{\mathrm{t}}_{\mathrm{tw}} - \mathrm{f}\left(1 + \frac{\mathrm{f} - 4\pi\,\mathrm{B}\,\mathrm{lk}}{2\,\mathrm{S}}\right) + \frac{1}{\lambda}\left(1 - \frac{\lambda}{4\,\mathrm{P_b}} - \frac{\lambda^2}{64\,{\mathrm{P_b}}^2}\right), \end{aligned} \tag{7.2}$$

with the twist free energy

$$\mathfrak{f}^{\mathrm{t}}_{\mathrm{tw}} \simeq 2\pi^2\,\mathrm{P_c}'\left\langle \mathrm{tw}^2 \right\rangle = 2\pi^2\,\mathrm{P_c}'\left(1 - \frac{\lambda\,\mathrm{P_c}'}{4\,{\mathrm{P_b}}^2}\right)\mathrm{lk}^2, \tag{7.3}$$

where we have added higher order terms from [172] to the free energy density. The values for the stretch modulus, $\mathrm{S} = 300\mathrm{nm}^{-1}$, and the stretch-twist coupling, $\mathrm{B} = -21$ we take from the recent paper by Sheinin and Wang [155]. The twist energy is one of the main results of Moroz et al. [172] who introduced the notion of the *thermally* renormalized torsional persistence length:

$$\mathrm{P_c^{eff}}(\lambda) = \left(1 - \frac{\lambda\,\mathrm{P_c}'}{4\,{\mathrm{P_b}}^2}\right)\mathrm{P_c}' \tag{7.4}$$

The linking number that was put into the chain gets spread between twist and a thermal writhe that is not symmetric around the straight twisted rod, but has a directionality thereby

decreasing the twist. The expectation value of this writhe per unit length, $\omega_{\text{tail}}^{\text{th}}$, and the resulting twist density, tw, are given by equation (6.14) or to lowest order as:

$$\left\langle \omega_{\text{tail}}^{\text{th}} \right\rangle = \frac{\mathrm{P_c}' \lambda}{4\,\mathrm{P_b}^2}\left(\mathrm{lk} + \frac{\mathrm{B\,f}}{2\pi S}\right) \Rightarrow \qquad \langle \mathrm{tw} \rangle = \mathrm{lk}\left(1 - \frac{\mathrm{P_c}' \lambda}{4\,\mathrm{P_b}^2}\right) - \frac{\mathrm{P_c}' \lambda\,\mathrm{B\,f}}{8\pi\,\mathrm{P_b}^2\,\mathrm{S}} \tag{7.5}$$

The thermal shortening with finite size correction follows from equation (6.15):

$$\begin{aligned}\rho_{\text{tail}} = 1 + \frac{\mathrm{f} - 2\pi\,\mathrm{B\,lk}}{\mathrm{S}} - \frac{1}{2\,\mathrm{K}}\left(1 + \frac{1}{64\,\mathrm{K}^2} + \cdots\right)\left(1 - \frac{\mathrm{B}}{2\,\mathrm{P_b\,S}}(2\pi\,\mathrm{lk\,P_c}' + \frac{\mathrm{B\,f}}{\mathrm{S}})\right) \\ + \left(\frac{1 - \coth(\frac{L_c\,\mathrm{K}}{\mathrm{P_b}})}{2\,\mathrm{K}} + \frac{\mathrm{P_b}}{2L_c\,\mathrm{K}^2}\right)\left(1 - \frac{\mathrm{B}^2\,\mathrm{f}}{2\,\mathrm{P_b\,S}^2})\right)\end{aligned} \tag{7.6}$$

The finite size correction differs from the correction given by [172] to make it valid for short chains, though the reasoning is the same. For a freely rotating WLC under tension the shortening factor is, up to quadratic order, given by [125]:

$$\rho_{\tau=0} = 1 - \frac{\coth(\frac{L_c\,\mathrm{K}_{\tau=0}}{\mathrm{P_b}})}{2\,\mathrm{K}_{\tau=0}} + \frac{\mathrm{P_b}}{2L_c\,\mathrm{K}_{\tau=0}^2} \tag{7.7}$$

As can be read of from K, the critical buckling bifurcation point gets shifted upwards to:

$$\mathrm{Lk}_{cr} = \frac{\mathrm{L_c}}{2\pi\,\mathrm{P_c}'}\left(2\sqrt{\mathrm{f\,P_b}} - \frac{\mathrm{B\,f}}{\mathrm{S}}\right) \tag{7.8}$$

The validity of these expressions is limited to values of force and linking number that make the expansion factor K large enough. Moroz and Nelson argued that for K^2 larger than 3, the error in the extension should be below 10%, based on a comparison with the next term in the asymptotic expansion. There are 2 other sources for errors: the appearance of knotted configurations, that should have been excluded from the partition sum and configurations with a writhe that differs a multiple of 2 from the calculated writhe caused by the use of Fuller's equation. For large K when large deviations from the straight rod are highly suppressed the influence of these effects are small and we will consider a value of $\mathrm{K}^2 = 3$ to be the lower bound below which the theoretical treatment of [172, 173] breaks down.

Once a plectoneme is formed one can think roughly of the solution as consisting of 3 distinct regions: the tails, where life is as in the straight pre buckling solution, the end-loop, and the plectoneme.

As was shown by Kulic et al [125], in a WLC under tension, it is the length of a loop, not the contour length of the chain forming the loop, that is to lowest order unaffected by thermal fluctuations. This has been shown for the case of a homoclinic parameter $t = 1$ loop with the two legs bound by a gliding ring at the contact point. There is no reason to doubt that this

will hold also for the end loops of the plectonemes, since they are sufficiently close to the closed loop, with the essential difference that the legs are not bound together but lie in an effective potential well resulting from a twist induced attraction and an electrostatic repulsion. Thermal fluctuations necessarily open the loop from its ground state value, thus decreasing its length. This loop destabilization effect becomes unimportant for a finite size plectoneme configuration, since loop opening and plectoneme radius are linked. To avoid unnecessary complications we will just ignore the entropic loop contributions and instead determine the relevant loop size from the plectoneme. The advantage of not having to introduce a detailed end loop entropic contribution to the free energy more than compensates for the small error it might produce in the free energy close to a possible plectonemeless loop configuration. In general it hardly affects the jump in length seen in the turn extension plots at the transition, since jumps indicate a finite size plectoneme at the transition.

The plectoneme part of the solution needs a more careful examination. As starting point we take the calculations by Ubbink and Odijk [153]. They considered one strand of the regular plectoneme fluctuating in the mean field potential of the opposing strand. They assume the fluctuations to have a Gaussian distribution around their average in two directions perpendicular to the strand. One direction is chosen pointing towards the opposing strand, the radial direction, the other normal to this direction, the pitch direction. Fluctuations in the radial direction are dominated by the exponent of the electrostatic interactions, while fluctuations in the pitch direction have much less influence on the energetics. Let us stress the advantage of this approach over expanding the effective confining potential around the ground state. In the radial direction the potential is highly skewed, exponentially increasing towards smaller radius. A harmonic approximation would only be valid in a tiny region around the ground state. Instead the point of view taken here is that the fluctuations are small compared to the typical length-scale of the chain, i.e. the persistence length. Denoting the standard deviation of the Gaussian distribution in the radial and pitch direction by respectively σ_r and σ_p, the electrostatic part of the free energy changes approximately to [153]:

$$\mathfrak{f}_{\mathrm{el}}(t,\alpha,\sigma_r) = \mathfrak{e}^0_{\mathrm{el}}\, e^{4\kappa^2\sigma_r^2} = \frac{\mathrm{q_{eff}}^2\, Q_B}{2}\sqrt{\frac{\pi}{\kappa R(t)}}e^{4\kappa^2\sigma_r^2-2\kappa R(t)}\, Z\left(\cot(\alpha)\right). \tag{7.9}$$

It is clear that the steep exponential rise of this free energy contribution limits the value of σ_r to be of order $(2\kappa)^{-1}$. This clearly distinguishes the magnitude of radial fluctuations from those in the "pitch-direction". It was argued in [178] that the standard deviation in the pitch direction should be of the order of the pitch itself. This one expects also purely on geometric grounds. The exact value is not that easy to calculate, but since it is considerably larger than the radial standard deviation, our results are fairly insensitive to its exact value, as it is the tightest direction that dominates the free energy of confinement (see below). In the following we will make the choice $\sigma_p = \pi R \sin(\alpha)$, which is the width of the virtual channel where a strand can move in perpendicular to the radial direction until it meets the opposing strand. The undulating chain contracts slightly with a factor ρ_{pl}, that we will discuss shortly. This

contraction decreases the bending energy density and the writhe density of the plectoneme per contour length in a nontrivial way. In appendix C.1 it is shown that they change to:

$$\mathfrak{e}_{\text{bend}} \to \mathfrak{f}_{\text{bend}} = {\rho_{\text{pl}}}^4\, \mathfrak{e}_{\text{bend}} = {\rho_{\text{pl}}}^4\, \frac{\mathrm{P_b}}{2} \frac{\cos^4(\alpha)}{R^2} \qquad \omega \to \rho_{\text{pl}}\, \omega = \rho_{\text{pl}}\, \frac{\sin(2\alpha)}{4\pi R} \tag{7.10}$$

For the entropic cost of confinement we cannot neglect the twist in the chain. The expectation value of the twist free energy density is, based on the equations of motion, constant along the chain. The space available to form thermal writhe in the plectoneme is in general not the same as for a straight chain under tension. And so we need to take the thermal writhe in the plectoneme explicitly into considerations. We now assign part of the total linking number to the tails and loop, from which follows a tension dependent expectation value of thermal writhe and twist density according to (7.5). The rest of the linking number has to be accounted for by the plectoneme. We use this difference as definition of its linking number. For a large part it is accounted for by the twist and the writhe of the zero temperature plectoneme, but some comes from the thermal writhe of the strands within the plectoneme. A problem is that writhe, as a local observable, is only defined with respect to a reference curve, which in our treatment thus far was the z-axis, not the writhing plectoneme. In appendix (C.1) it is shown that under reasonable assumptions the thermal writhe can be treated as an additive correction to the plectoneme writhe, where the thermal writhe is calculated as the thermal writhe of an undulating chain, with a finite linking number, confined in a straight channel. For the calculation of the relevant quantities for a torsionally constrained confined WLC we can fall back to Section 6.3.2. The two directions x, y in equation (6.75) are the radial and pitch directions of the plectoneme strands. We assume we can capture the physics of confinement of the plectoneme strands with that of a harmonic confined chain with the same standard deviations σ_r and σ_p. In other words: the transversal distribution is Gaussian enough. In that case are the confinement free energy, the contraction factor and thermal writhe density given by equation (6.76). After inclusion of the twist factor multiplying the fluctuation determinant we find to lowest order for the free energy of the plectoneme strands

$$\mathfrak{f}_{\text{strand}} = \mathfrak{f}_{\text{tw}}^{\text{str}} + \frac{3}{8}\left(\frac{1}{\lambda_r} + \frac{1}{\lambda_p}\right) \tag{7.11}$$

$$\text{with } \mathfrak{f}_{\text{tw}}^{\text{str}} := 2\pi^2\, \mathrm{P_c}'\left\langle {\mathrm{tw_{str}}}^2 \right\rangle = 2\pi^2\, \mathrm{P_c^{eff}}(\bar{\lambda})\, {\mathrm{lk_{str}}}^2, \tag{7.12}$$

where $\mathrm{P_c^{eff}}()$ is the function of λ as given by equation (7.4) The relative extension of the chain is to the same order given by

$$\rho_{\text{pl}} = 1 - \frac{2\,\mathrm{B\,lk_{str}}}{\mathrm{S}} - \frac{1}{4}\left[\frac{\lambda_r}{\mathrm{P_b}} + \frac{\lambda_p}{\mathrm{P_b}}\right] + \frac{2\lambda_s\, \mathrm{B}\, \pi\, \mathrm{P_c}'\, \mathrm{lk_{str}}}{\mathrm{S}\, {\mathrm{P_b}}^2} \tag{7.13}$$

It is important to stress that the confinement free energy is purely entropic: the contribution of the confining potential was subtracted from the full free energy. The confining channel in

the plectoneme is not straight and the r and p directions rotate around the channel axis. This does influence the writhe. The length scale of these is of the order of the pitch or, as argued above, of the standard deviation, in that channel direction. In all cases we consider, the radial standard deviation is considerably smaller than that in the pitch direction. As can be seen from the equations, the torsional deflection length ranges in that case from $\bar{\lambda} = 3\lambda_r/2$ for $\sigma_r = \sigma_p$, till $\bar{\lambda} \simeq 2\lambda_r$ for $\sigma_r \ll \sigma_p$. Since this is the length scale where confinement dominates thermal fluctuations, as long as it is much smaller than the pitch, the global writhing path is not affected by thermal fluctuations. The contraction ρ_{pl} does depend somewhat on fluctuations in the pitch direction and so its size does affect plectoneme formation to some extend. The free energy density of the plectoneme is the sum of this confinement-, the bending (7.10)- and electrostatic (7.9) free energy:

$$\mathfrak{f}_{\mathrm{plect}} = \mathfrak{f}_{\mathrm{bend}} + \mathfrak{f}_{\mathrm{strand}} + \mathfrak{f}_{\mathrm{el}} \tag{7.14}$$

The energy stored in the twist is expected to have a fast relaxation time, since twist hardly couples to the environment. Experiments confirm this [179]. Therefore the twist free energy density is equal in the tails and the plectoneme strand. Since the magnitude of the fluctuations is not necessarily the same, the expectation values of the twist will in general differ. Equating $\mathfrak{f}_{\mathrm{tw}}^{\mathrm{t}}$ and $\mathfrak{f}_{\mathrm{tw}}^{\mathrm{str}}$ allows us to eliminate the linking density of the strands in the plectoneme as parameter and write $\mathrm{lk}_{\mathrm{str}} = \delta\,\mathrm{lk}$, with

$$\delta = \sqrt{\frac{\mathrm{P}_{\mathrm{c}}^{\mathrm{eff}}(\lambda)}{\mathrm{P}_{\mathrm{c}}^{\mathrm{eff}}(\lambda_s)}} \tag{7.15}$$

close to one by assumption. This is indeed the case in all experimental conditions studied: For forces ranging from 0.5 pN to 4 pN, λ varies from 7 nm to 20 nm, leading to an effective torsional persistence length of $\mathrm{P}_{\mathrm{c}}^{\mathrm{eff}}(\lambda) \simeq (0.8-0.93)\,\mathrm{P_c}'$. On the other hand the radial standard deviation in the plectoneme is largely set by the Debije screening length. With monovalent salt concentrations in the range of 20 mM to 320 mM and assuming $\sigma_r \simeq \kappa^{-1}/2$ we can estimate the corresponding effective persistence length to be $\mathrm{P}_{\mathrm{c}}^{\mathrm{eff}}(\lambda_s) \simeq (0.91 - 0.96)\,\mathrm{P_c}'$, and so a crude estimate for δ is $1.01 \geq \delta \geq 0.91$. Although the difference in 'thermal waste' while transforming linking number into twist is rather small, it would be wrong to draw the conclusion that entropic effects can be neglected, since the entropic part of the free energy goes as $\simeq \mathrm{k_B T}/\lambda$. The difference between the two states can be up to one $\mathrm{k_B T}$ per nm.

It is worthwhile to split off the twist contribution to the free energies:

$$\left.\begin{matrix}\mathfrak{f}_{\mathrm{tail}} \\ \mathfrak{f}_{\mathrm{plect}}\end{matrix}\right\} = \mathfrak{f}_{\mathrm{tw}} + \left\{\begin{matrix}\mathfrak{g}_{\mathrm{tail}} \\ \mathfrak{g}_{\mathrm{plect}}\end{matrix}\right. \tag{7.16}$$

with:

$$\mathrm{g_{tail}} = -\mathrm{f}\left(1 + \frac{\mathrm{f} - 4\pi B\,\mathrm{lk}}{2\,\mathrm{S}}\right) + \frac{1}{\lambda}\left(1 - \frac{\lambda}{4\,\mathrm{P_b}} - \frac{\lambda^2}{64\,{\mathrm{P_b}}^2}\right) \tag{7.17}$$

$$\mathrm{g_{plect}} = \frac{3}{8}\left(\frac{1}{\lambda_r} + \frac{1}{\lambda_p}\right) + \mathrm{f_{bend}} + \mathrm{f_{el}} \tag{7.18}$$

the remaining free energy contributions. We will use $\Delta\mathrm{g} = \mathrm{g_{plect}} - \mathrm{g_{tail}}$ to denote their difference. Once a plectoneme has formed the expectation value of its contour length follows from the combined linking numbers of plectoneme and end-loop, which should add to the linking number that was externally applied:

$$\mathrm{Lk} = (\mathrm{L_c} - \mathrm{L_p})\,\mathrm{lk} + \mathrm{L_p}[\rho_{\mathrm{pl}}\,\omega + (1-\epsilon)\,\mathrm{lk}] + \mathrm{Wr_{loop}} \Rightarrow \quad \mathrm{l_p} := \frac{\mathrm{L_p}}{\mathrm{L_c}} = \frac{\nu - \mathrm{lk} - \mathrm{Wr_{loop}}\,/\,\mathrm{L_c}}{\rho_{\mathrm{pl}}\,\omega - \epsilon\,\mathrm{lk}}, \tag{7.19}$$

with $\nu := \mathrm{Lk}\,/\,\mathrm{L_c}$ the applied linking number density. The reduced free energy density of this one plectoneme configuration and its extension are:

$$\begin{aligned} \mathrm{f}_1 &= (1 - \mathrm{l_p})\,\mathrm{f_{tail}} + \mathrm{l_p}\,\mathrm{f_{plect}} \\ &= \mathrm{f_{tw}} + \mathrm{g_{tail}} + \mathrm{l_p}\,\Delta\mathrm{g} + \frac{\mathfrak{E}_{\mathrm{loop}}(t)}{\mathrm{k_B T\,L_c}} \end{aligned} \tag{7.20}$$

$$\frac{\Delta z}{\mathrm{L_c}} = \rho_{\mathrm{tail}}(1 - \mathrm{l_p}) - \frac{\mathrm{L_{loop}}}{\mathrm{L_c}} \tag{7.21}$$

both depending on the 4 parameters R(or t),σ_r, α and lk. The calculation boils down to a 4 parameter minimization procedure. In the long chain limit with finite plectoneme length the loop contribution can be neglected in determining the 4 parameters. We can assume that ϵ is small compared to ω, under conditions where a plectoneme forms. We can also neglect the dependence of ρ_{pl} on the parameters, its variational contribution is on the order of $\lambda_{r,p}/\,\mathrm{P_b}$, which is small by assumption. The long chain finite plectoneme free energy is:

$$\mathrm{f}_1 = \mathrm{f_{tw}}(\mathrm{lk}) + \mathrm{g_{tail}} + \frac{\nu - \mathrm{lk}}{\rho_{\mathrm{pl}}\,\omega(R,\alpha)}\,\Delta\mathrm{g}(R, \alpha\sigma_r) \tag{7.22}$$

The linking number density and chain extension are readily obtained in this limit:

$$\mathrm{lk} = \frac{\Delta\mathrm{g}}{4\pi^2\,{\mathrm{P_c}}'\,\rho_{\mathrm{pl}}\,\omega(R,\alpha)} \qquad\qquad \frac{\Delta z}{\mathrm{L_c}} = -\frac{\rho_{\mathrm{tail}}}{\rho_{\mathrm{pl}}\,\omega(R,\alpha)} \tag{7.23}$$

Minimizing the free energy is within this approximation equivalent to minimizing the linking number density. This is not really a surprise since plectoneme formation is driven by linking number. A numeric minimization gives results that compare in general well with experiments

only under limited conditions, namely the transition point, height of the jump at the transition as well as the slope after the transition are within experimental error for high enough forces and salt concentrations, see Figure 8.1. The lack of agreement clearly inversely correlates with K^2. Dropping the assumption of equal linking number densities in tail and plectoneme hardly improves the results. Especially for low salt concentrations the agreement is good only for a small range of relatively high forces, even when the value of K^2 stays well above 3. This discrepancy, that is slightly stronger when fluctuations are neglected, has led to a variety of speculations: an effective charge reduction [150], partly introduced to explain torques measurements, and a charge correlation effect between the two intertwined super-helices that form the plectoneme [177]. The deviation of the experimental slopes from the calculated one goes hand in hand with the decrease of the height of the potential barrier between straight and plectoneme configuration. But our theory is not complete yet: the inclusion of other local minima next to these two configurations turns out to be of greater importance than has been acknowledged until now, as we will show in the next section.

7.2 Instantons

Contributions of local minima have to be taken separately into account in any perturbative calculation. A standard way to grasp their influence in statistical as well as quantum physics is through the concept of an instanton. Using the picture of a particle moving in an inverted potential, in our case the Kirchhoff analogy, the transition can be seen as a fast jump from one (local) minimum to another, fast since the particle in the inverted potential converts potential energy into kinetic energy during the tunneling through the barrier.

The usual way to take these local minima into account is to treat them as a gas of defects that compete with their entropic gain against the energetic advantage of the ground state. This is the situation that would exist in a torque regulated setup. In our case where the linking number is the control parameter the treatment changes essentially. A defect changes the linking number and so the energy of the configuration in which it is embedded. Furthermore the defects are themselves plectonemes and so to understand thermal fluctuation close to the transition we actually study multi-plectoneme configurations.

The entropic gain of a multi-plectoneme configuration is twofold: there is the usual combinatoric positional freedom of defect placement (the "gas of defects"), but there is also an increase in configurations due to the freedom in distributing the total plectoneme length over the individual plectonemes. Treating the plectonemes as having a hardcore repulsion, one finds for the density of states of a configuration with *total* plectoneme contour length L_p spread out over m plectonemes:

$$z_m = \frac{1}{\Lambda^{2m-1}} \frac{{L_p}^{m-1}(m)}{(m-1)!} \frac{(L_c - m\, L_{loop} - L_p(m))^m}{m!}, \tag{7.24}$$

with Λ a cutoff scale that we will take to be the helical repeat. This expression can be easily derived using Laplace transforms (see Appendix C.2). The result is essentially the product of the two contributions: the first fraction counts the possible ways to distribute the plectoneme length over the m plectonemes, while the second fraction counts the number of ways the gas of defects, in the guise of end-loops, can be partitioned over the free chain length. The choice of cutoff, is a choice of the unit we count in. The m dependent plectoneme length follows as before from the total linking number.:

$$\mathrm{L_p}(m) = \mathrm{L_c}\,\frac{\nu - \mathrm{lk} - m\,\mathrm{Wr_{loop}}\,/\,\mathrm{L_c}}{\rho_{\mathrm{pl}}\,\omega - \epsilon\,\mathrm{lk}} \tag{7.25}$$

We cannot drop the loop contribution here since we should leave the possibility open that the number of plectonemes increases at the same (or higher) rate as the contour length. For the same reason we should also take the end-loop energy term into account. In principle also plectonemes with a negative writhe should be included. Their contribution is very small except when tension and linking number are low. We are mainly interested in linking numbers around and above the bifurcation point. In the following we will neglect them.

The maximum number of plectonemes can never be higher than $\mathrm{L_c}\,/\,\mathrm{L_{loop}}$ and it is to be expected that finite size effects easily dominate the turn extension curves for shorter chains. We want to describe the generic behavior of the turn extension plot without end effects. The reason is not only to avoid plectoneme-plectoneme interactions, but also to avoid interactions of the magnetic/optical bead with the substrate and details of the exact geometry of attachment of the chain ends. It is sensible to work again in the large $\mathrm{L_c}$ limit, above the bifurcation point but with small enough linking number that the plectoneme density is low. These demands translate to $\mathrm{L_p} > 0$ and $\mathrm{L_c} \gg m\,\mathrm{L_{loop}} + \mathrm{L_p}$. Taking $\epsilon = 0$ and $\rho_{\mathrm{pl}} = 1$ we write the free energy of the chain as:

$$\mathcal{F} = \mathrm{L_c}\,\mathfrak{f}_0 + m\Delta = \mathrm{L_c}(\mathfrak{f}_0 + \frac{\mu}{\mathrm{L_{loop}}}\Delta) \qquad \text{with } \Delta = \mathfrak{E}_{\mathrm{loop}} - \frac{\mathrm{Wr_{loop}}\,\Delta\mathrm{g}}{\omega} \tag{7.26}$$

with $\mathfrak{f}_0$ collecting the terms of the free energy density, that do not depend on the *loop density* $\mu := m\,\mathrm{L_{loop}}\,/\,\mathrm{L_c}$. Since Δ is larger than zero iff the energetic cost per writhe of the loop is larger than that of the plectoneme, a negative delta results in a plectonemeless chain where the excess linking number is distributed over loops with writhe density $\omega_l := \frac{\mathrm{Wr_{loop}}}{\mathrm{L_{loop}}}$. Only entropic effects can change this. One caveat: close to the zero length plectoneme the lack of a proper electrostatic model for the endloop influences the free energy too much. This is not that serious when using plectoneme parameters in the long chain, finite plectoneme limit, but distorts the transition to some degree. To simplify the following discussion we will treat the cutoff and the loop length as being the same. The error amounts to logarithmic corrections that will have no influence on the conclusions we will draw. Comparing in the next chapter the model with experiments the change of cutoff has an effect smaller than the experimental error in all experiments we compared the model with. The loop density, μ, dependence of the

partition sum is now:

$$Z \sim \int_0^{\mu_m} \mathrm{d}\mu \exp\left\{\frac{\mathrm{L_c}\,\mu}{\mathrm{L_{loop}}}\left[\log\left(\frac{\mathrm{l_p}(\mu)}{\mu}\frac{(1-\mu-\mathrm{l_p}(\mu)}{\mu}\right)+2-\Delta\right]\right\}$$
$$\simeq \int_0^{\mu_m} \mathrm{d}\mu \exp\left\{\frac{\mathrm{L_c}\,\mu}{\mathrm{L_{loop}}}\left[\log\left(\frac{\mathrm{l_p}(\mu)}{\mu^2}\right)+2-\Delta\right]\right\}, \quad (7.27)$$

with μ_m the maximum density set by $\mu_m = \sup\{\mu \in [0,1] | 0 \leqq \mathrm{l_p}(\mu) \leqq 1-\mu\}$. The extension of the chain can be seen as having two contributions: one from the plectoneme(s) and one from the loops:

$$\frac{z}{\mathrm{L_c}} = 1 - \mathrm{l_p} - \mu \quad (7.28)$$

It is straight forward to verify that the argument of the resulting exponent is a concave function of μ for $\mu \in (0, \mu_m)$ and so its dominant contribution comes from it's maximum:

$$\log\left(\frac{l_p(\langle\mu\rangle)}{\langle\mu\rangle^2}\right) - \frac{\langle\mu\rangle\,\frac{\omega_{\mathrm{loop}}}{\omega}}{l_p(\langle\mu\rangle)} - \Delta = 0 \quad (7.29)$$

Since the two last terms are negative we should have $l_p(\langle\mu\rangle) > \langle\mu\rangle^2$. Single plectoneme behavior is to be expected when $l_p \simeq \frac{\nu-\mathrm{lk}}{\omega}$. When this is the case:

$$\langle\mu\rangle \simeq \sqrt{\frac{\nu-\mathrm{lk}}{\omega}}e^{-\Delta/2} \ll \frac{\nu-\mathrm{lk}}{\omega_{\mathrm{loop}}} \Rightarrow \frac{\nu-\mathrm{lk}}{\omega} \gg \left(\frac{\omega_{\mathrm{loop}}}{\omega}\right)^2 e^{-\Delta} =: \zeta \quad (7.30)$$

Of course multiple plectonemes do always appear for long enough chains. Their appearance normally does not change the slope of the turns extension plot in a measurable way. Once the nucleation of plectonemes dominates the slope we speak of a multi plectoneme phase. The right hand side of (7.30), the *multi plectoneme* (MP) factor, ζ, is an indicator for the multi plectoneme phase. We can distinguish 2 contributions that suppress multi-plectonemes: a large loop energy per gained writhe as compared to the plectoneme and and a low writhe density in the loop, compared to the plectoneme. This last contribution is of purely entropic origin. The behavior of the multi-plectoneme factor is depicted in 7.1. The largest factor is at low salt and high tension. We can understand the curve by realizing that the plectoneme radius depends differently on force or salt concentration depending on their strength. The loop writhe density, which is on the order of $1/(4\lambda)$, is almost independent of the salt concentration, since the homoclinic parameter varies over a small range. At low salt ω is of the order κ. This is partly due to the electrostatics stabilizing the plectoneme opening angle to a value that is almost constant over a large range of conditions, while the plectoneme radius is to a large extend determined by the electrostatic interactions, resulting in a radius of the order of the Debije length. Since the writhe density of the plectoneme scales as $1/R$ we find $\omega \sim \kappa$. The

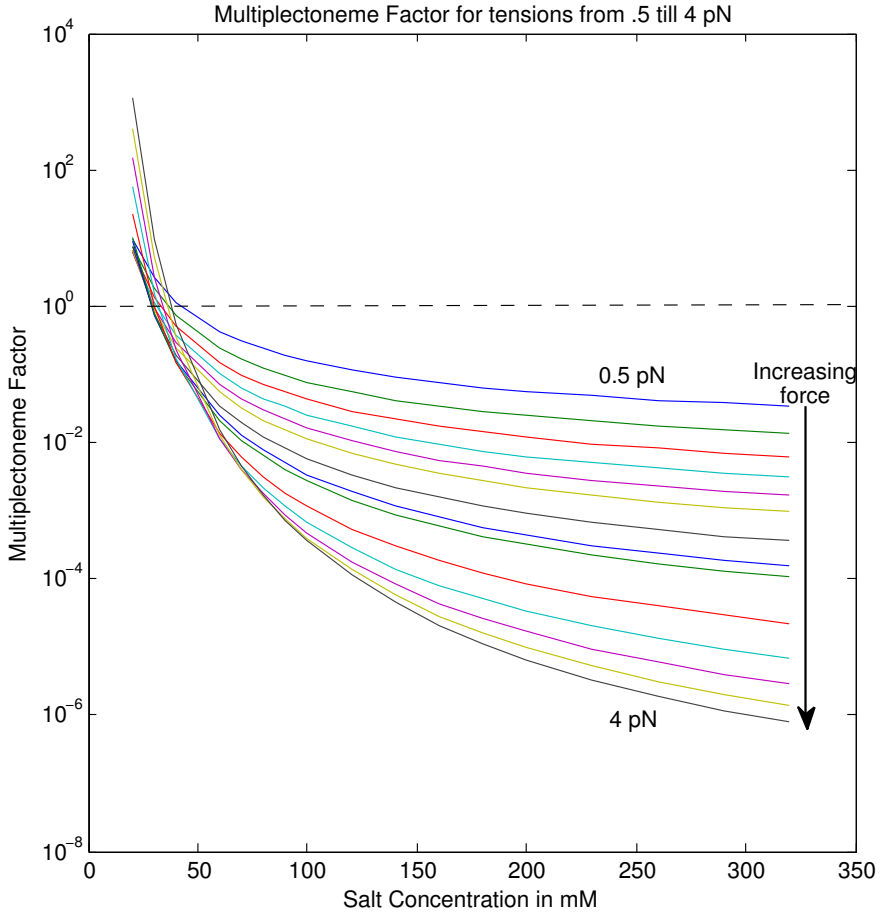

Figure 7.1: Multi-plectoneme factor

ratio $\omega_{\text{loop}} \,/\, \omega$ increases with decreasing salt concentration. Since the plectoneme free energy density at the same time increases while the loop energy stays roughly constant, Δ decreases and thus the MP factor increases. An increasing tension at a constant low salt concentration increases the pre-factor that scales as $\mathrm{f} \,/\, \mathrm{P_b}$. At the same time the loop energy increases as $\sqrt{\mathrm{f}\,\mathrm{P_b}}$ but the plectoneme contribution to Δ ($\Delta \mathrm{g} \,/\, \omega$) increases almost linearly with f since R's dependence on f is small.

This behavior changes at higher salt concentrations where it is the deflection length λ that sets the plectoneme radius resulting in an almost constant pre-factor and a Δ that increases as $\sim \sqrt{\mathrm{f}\,\mathrm{P_b}}$. This results in a decreasing MP factor with increasing tension.

A multi-plectoneme state corresponds to a linear dependence of $\mu \simeq \frac{\nu - \mathrm{lk}}{\omega_l}$. Since $\omega_{\text{loop}} < \omega$ we expect an increase of the slope due to multi-plectonemes. The slope naturally splits into a

one plectoneme contribution and an MP contribution as follows:

$$-\frac{\partial_\nu z}{L_c} = \frac{1}{\omega} + \partial_\nu \mu \left(1 - \frac{\omega_{\text{loop}}}{\omega}\right). \tag{7.31}$$

By lowering the salt concentration it is possible to arrive at a situation that the writhe density of the loop is larger than that of the plectoneme, while the plectoneme is still energetically favorable. An overall picture of the MP phase is clarified by the contour plot, Figure 7.2, of

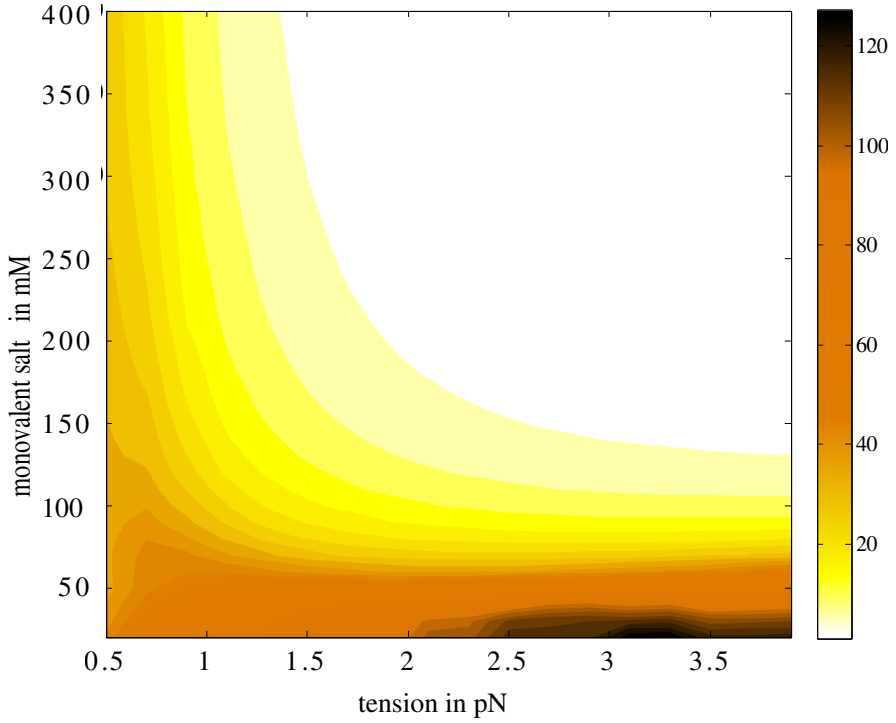

Figure 7.2: Contourplot of the number of plectonemes as function of salt concentration and tension for a 7.2 µm long chain

the number of plectonemes for a chain of 7.2 µm as it varies over a range of combinations of tension and salt concentration.